Available online at www.sciencedirect.com
SCIENCE DIRECT®
Surface Science 540 (2003) 230–236
SURFACE SCIENCE
www.elsevier.com/locate/susc

Overpotential deposition of Ag monolayer and bilayer on Au(1 1 1) mediated by Pb adlayer underpotential deposition/stripping cycles

J.X. Wang [a,*], B.M. Ocko [b], R.R. Adzic [a]

[a] Department of Materials Science, Brookhaven National Laboratory, Building 555, Upton, NY 11733, USA
[b] Department of Physics, Brookhaven National Laboratory, Upton, NY 11973, USA

Received 27 February 2003; accepted for publication 31 May 2003

Abstract

Ultra-thin Ag films on the Au(1 1 1) surface were prepared via overpotential deposition (OPD) in the presence of Pb^{2+} ions. By carrying out repetitive Pb adlayer underpotential deposition (UPD) and stripping cycles during Ag bulk deposition, the two-dimensional growth of Ag films was significantly enhanced in high OPD. The Ag monolayer sample was made by comparing the voltammetry curves, in which the signatures for Pb adlayer UPD on Au(1 1 1) changed to that on Ag(1 1 1). As demonstrated by the X-ray specular reflectivity measurements, nearly complete monolayer and bilayer films can be made with optimized deposition procedures. On subatomic scale, however, we found that these films have significant higher root-mean-square displacement amplitudes than those underpotentially deposited Ag monolayer and bilayer on either Au(1 1 1) or Pt(1 1 1).

Keywords: Growth; Surface structure, morphology, roughness, and topography; X-ray scattering, diffraction, and reflection

1. Introduction

The growth of smooth layers of one material on foreign substrates has long been an important goal of surface science investigations. It has been found that incorporating certain metal atoms during the deposition process can promote layer-by-layer growth, yielding smooth deposits [1,2]. For example, three-dimensional (3D) island formation of Ge on Si(1 1 1) [3] or Ag on Ag(1 1 1) [4] can be altered to a layer-by-layer growth mode by adding Sb, which acts as a surfactant. Alternatively, the 2D growth of Ag thin films on Ag(1 1 1) can be induced by ion bombarding the surface with low-energy Ar^+ pulses, thereby creating defects [5]. Both procedures, adding surfactant and creating defects, are believed to enhance the nucleation density and/or reduce the magnitude of the edge barrier so that the interlayer transport of deposited adatoms is rapid enough to prevent nucleation of islands on the as yet uncompleted growing monolayers.

Applying the results of the vacuum studies of surfactant and defect mediated growth to electrodeposition, Sieradzki et al. demonstrated that the

* Corresponding author. Tel.: +1-631-344-2515; fax: +1-631-344-5815.
E-mail address: jia@bnl.gov (J.X. Wang).

0039-6028/$ - see front matter © 2003 Elsevier B.V. All rights reserved.
doi:10.1016/S0039-6028(03)00792-1

2D growth of Ag on Au(1 1 1) can be achieved by using either lead or copper as the mediator [6]. Similar effects have also been observed in the electrodeposition of Au in the presence of lead [7] and antimony [8] ions. Although the scanning tunneling microscopy (STM) images provided a clear picture for the evolution of surface morphology during the deposition of hundreds of monolayers [6], an important unresolved issue has been whether ultra-thin films exhibit layer-by-layer growth. Can a monolayer or bilayer film be electrodeposited by using these methods in the overpotential deposition (OPD) regime? The answer will lead to a better understanding on an atomic scale of this growth, and the method may be applied in electrocatalysis. In the latter case, the formation of a complete monolayer or bilayer is interesting because electronic effects on catalytic properties, due to the interaction between the admetal and substrate, decay with the film thickness rather rapidly.

It is well known that for certain metals monolayer or bilayer films can be deposited on many noble metal surfaces at potentials positive of the bulk deposition potential. This occurs when the admetal–substrate bonding is stronger than admetal–admetal bonding and is referred to as the underpotential deposition (UPD). In some cases, the UPD metal thin films exhibit properties differing from the pure metals of either the admetal or the substrate, depending on the film thickness. For example, the Ag monolayer on the Pt(1 1 1) surface adsorbs bisulfate ions in a manner similar to the Pt(1 1 1) surface, while the Ag bilayer adsorbs sulfate in a manner similar to the Ag(1 1 1) surface [9]. Modification of surface properties through thin film deposition is thus of a great interest for electrocatalysis [10]. Since the UPD of a foreign admetal is a thermodynamic property, it is not always applicable. Therefore, a general method of metal adlayer growth, based on kinetic rather than thermodynamic factors, which may be applicable to a wide range of systems where UPD is not a viable option, is of a considerable interest.

In this paper, we describe a deposition procedure for controlled making of well ordered Ag monolayers and bilayers on the Au(1 1 1) surface at potentials far below the Ag bulk deposition potential. It involves the use of Pb UPD/stripping potential cycles to modify the growth kinetic of the Ag film. Since Ag monolayer and bilayer can be formed by UPD on Au(1 1 1) [11,12], the procedure itself may not have much practical value. Our goal in this X-ray reflectivity study is using it as an example to explore the potential of kinetic controlled 2D growth for ultra-thin film. The system is chosen because the monolayer formation can be monitored in situ by using the Pb UPD voltammetry feature and Ag deposits can be easily removed from gold so that various deposition procedures can be tested in reasonable time. Unlike microscopic scanning techniques, which monitor the microscopic surface morphology during the deposition, X-ray reflectivity measurements, as a global probe for atomic distribution along the surface normal direction, are taken after a certain amount deposition is made. A layer-by-layer growth is judged by whether only one monolayer is found when the whole surface is fully covered by Ag, and whether a bilayer forms when the amount of deposit is twice as much as that for a monolayer. This is more strict definition than that based on the lack of small clusters and multi-atomic height islands in STM images. On the basis of this definition, we found that a kinetic controlled Ag layer-by-layer OPD on Au(1 1 1) can be achieved under optimized conditions, probably only up to two monolayers.

2. Experimental

The Au(1 1 1) single crystal (10 mm in diameter), was electropolished after orientation within 0.15 °C of the crystalline direction. The crystal was flame annealed and cooled to below 100 °C when a drop of MilliQ UV-plus (Millipore) water was placed on to the crystal surface. The water drop protected the surface from contamination during the transfers to an electrochemical cell. A Ag/AgCl/(3 M NaCl) electrode was used as the reference electrode and a Pt wire was used as the counter electrode. All potentials reported here have been referenced to the normal hydrogen electrode (NHE). Solutions were prepared from Ag_2SO_4, PbO (99.999%, Aldrich), and ultra-pure $HClO_4$.

A hanging meniscus configuration was used in voltammetry measurements and for controlled electrodeposition of Ag in the presence of Pb^{2+} ions. After Ag electrodeposition, the crystal was removed from the solution underpotential control, dipped into Millipore water, and then transferred to the X-ray cell with a drop of water on top of the crystal surface. This sample transfer procedure has been verified in our previous works using Ag single crystals to be effective to prevent Ag surface oxidation in air. Using this procedure, instead of depositing Ag in the X-ray cell, ensured that the change of the fine feature in the voltammetry curve during Ag deposition could be observed clearly and used for monitoring the amount of Ag deposited. After sealing the X-ray cell with a thin plastic window, the cell was filled with deoxygenated water. An outer chamber was filled with nitrogen gas to keep the cell free of oxygen during the measurements. Under these conditions, repeated measurements show no change of measured X-ray intensity with time.

X-ray specular reflectivity measurements were performed at beam line X22A with $\lambda = 1.20$ Å at the National Synchrotron Light Source. Following convention, a hexagonal coordinate system was used for the Au(1 1 1) crystal in which the reciprocal-space vector along the surface direction was $Q_z = Lc^*$, where $c^* = 2\pi/c$ and $c = 7.064$ Å. A 2×2-mm detector slit was located 650 mm from the sample.

3. Results and discussion

Linear sweep voltammetry curves for Ag UPD and OPD on Au(1 1 1) in $HClO_4$ solution containing 0.1 mM Ag^+ ions without and 10 mM Pb^{2+} ions are shown in Fig. 1. A low Ag^+ concentration was chosen to make the rate of OPD of Ag slow. The current peaks at potentials positive of 0.563 V are due to the UPD of Ag. These peaks are not as sharp and symmetric as the literature data [13,14], obtained at higher concentrations where there is no diffusion limitation for Ag deposition. The presence of Pb^{2+} ions gives rise to the additional peaks close to zero volts. These features are similar to those observed for the case of the Pb UPD

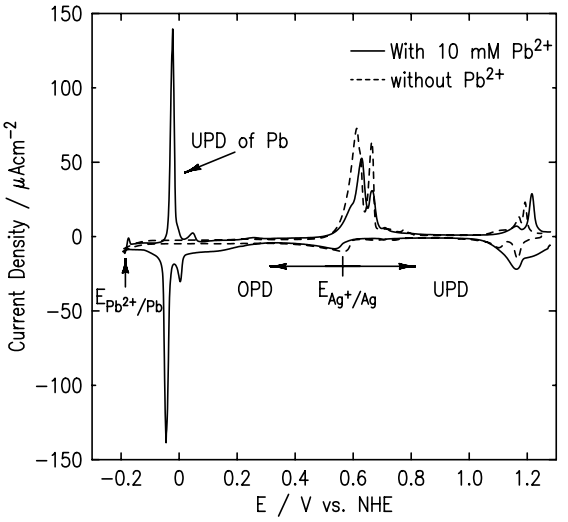

Fig. 1. Linear sweep voltammetry curves for Au(1 1 1) in 0.1 M $HClO_4$ containing 0.1 mM Ag^+ with (solid line) and without (dashed line) 10 mM Pb^{2+}. Sweep rate 10 mV/s.

peaks on Au(1 1 1) [15]. The smaller bulk Ag stripping peak, compared to that one in the absence of Pb, indicates that the presence of the Pb decreases the rate of Ag deposition.

Fig. 2 shows the voltammetry curves obtained for the OPD of Ag monolayer and bilayer on a freshly prepared Au(1 1 1) electrode in 0.1 M $HClO_4$ solution containing 0.1 mM Ag^+ ions and 10 mM Pb^{2+} ions. To mediate and control the 2D growth of Ag monolayer in OPD potential region, the electrode potential was continuously cycled at 30 mV/s between −0.1 (or −0.08 V) and 0.1 V, a potential range where the Pb monolayer is alternatively deposited and removed. The potential cycling was initiated at a potential just negative of the UPD features and reversed at a potential where the Pb UPD layer is completely stripped. As shown in Fig. 2a, whereas the current peaks at higher potential decrease with cycling, the low-potential current peaks increase with the number of cycles. Since the small Pb UPD peak at higher potential occurs on Au(1 1 1), but not on Ag(1 1 1), the decrease of this pre-peak and the increase of the major peak at lower potential indicate that the Au(1 1 1) surface becomes gradually covered by Ag. When the peak at higher potential vanished (after about the thirteenth positive potential

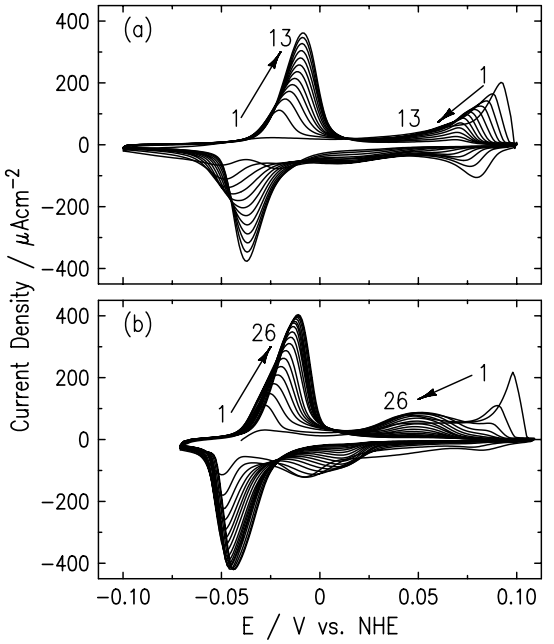

Fig. 2. (a) Linear sweep voltammetry curves showing the decrease of the high potential peak and the increase of the low potential peak during the overpotential deposition of a Ag monolayer on Au(1 1 1) mediated by repeated Pb UPD/stripping potential cycles in 0.1 M $HClO_4$ containing 0.1 mM Ag^+ and 10 mM Pb^{2+}. Sweep rate 30 mV/s. (b) Voltammetry curves recorded during formation of the Ag bilayer sample, which was carried out under the same condition as for the monolayer with the number of potential cycles doubled.

sweep) the electrode was disconnected, rinsed with pure water, and transferred to the X-ray cell for the X-ray specular reflectivity measurement. Samples for monolayer deposition were also made by potential cycling at 10 and 50 mV/s, or by pulsing potential between −0.1 and 0.1 V. The most complete and flat monolayer was obtained by the potential cycles at 30 mV/s, as described above. For the bilayer sample, as shown in Fig. 2b, the number of potential cycles was 26, twice as many as that for the monolayer deposition.

The specular reflectivity profiles obtained for the monolayer and bilayer Ag deposits on Au(1 1 1) are shown in Figs. 3 and 4. Both curves show distinct features between the Bragg peaks that are different from those obtained for the ideally terminated Au(1 1 1) surfaces. In the kinematic approximation, the specular reflectivity is related to

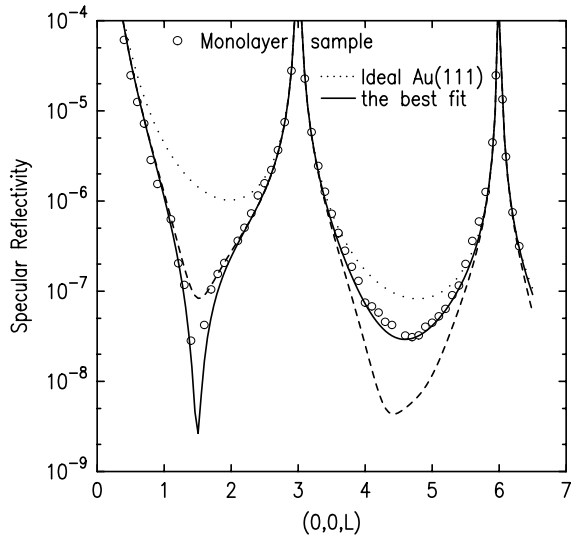

Fig. 3. X-ray specular reflectivity profile for the Ag monolayer on a Au(1 1 1) electrode. The dotted line is calculated for an ideal Au(1 1 1) surface. The solid line shows the best fit and the dashed line is calculated as described in the text.

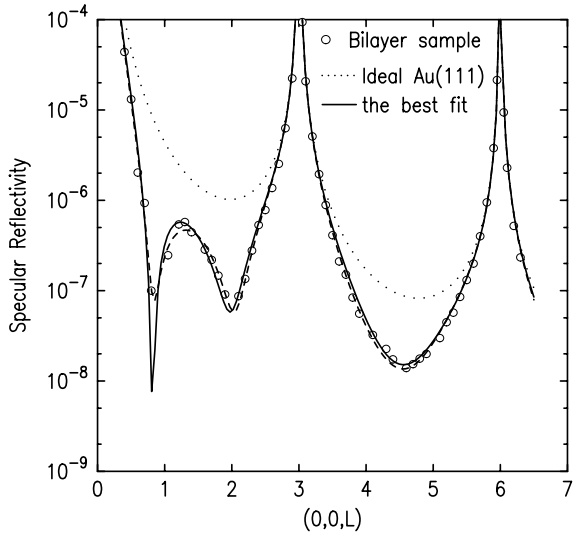

Fig. 4. X-ray specular reflectivity profile for the Ag bilayer on a Au(1 1 1) electrode. The dotted line is calculated for an ideal Au(1 1 1) surface. The solid and dashed lines are the fits described in the text.

the sum over atomic layers with the appropriate atomic form and phase factors for each layer. In our model, the scattering factor for the surface

layers incorporates a nearly ideally terminated Au(1 1 1) surface with up to three adlayers, given by

$$F(L) = f_{\mathrm{Au}}(L)\mathrm{e}^{-q^2\sigma_0^2/2}\mathrm{e}^{2\pi\mathrm{i}LZ_0} + \sum_{j=1}^{3}\theta_j f_j(L)\mathrm{e}^{-q^2\sigma_j^2/2}\mathrm{e}^{2\pi\mathrm{i}LZ_j/c}, \quad (1)$$

where f is atomic factor and q is the reciprocal-space vector along the surface direction, which is equal to $2\pi L/c$ with $c = 7.064$ Å for Au(1 1 1). The adjustable parameters are the layer spacings represented by the position along the surface normal direction, Z_j, the vertical root-mean-square (rms) displacement amplitudes, σ_j, and the coverage with respect to the atomic density of the Au(1 1 1) surface, θ_j. The density of the top Au layer is fixed at unity because we have checked by in-plane diffraction that the Au(1 1 1) surface reconstruction is lifted by Pb UPD.

For the monolayer sample, as shown in Fig. 3, the measured specular reflectivity is well reproduced (solid line) with one nearly complete Ag monolayer (i.e., $\theta_1 = 0.98$ and $\theta_2 = \theta_3 = 0$). Other fitted parameters are the Ag–Au layer spacing ($Z_1 - Z_0 = 2.36$ Å), the top Au layer spacing ($Z_0 = 2.35$ Å) and the rms amplitudes for the Ag adlayer ($\sigma_1 = 0.45$ Å) and the top Au layer ($\sigma_0 = 0.14$ Å). Since X-ray reflectivity measures the electron density profile along the surface normal direction, and hence is not directly atomic sensitive, there are unlimited possibilities for a mixed Ag–Pb adlayer to have the electron density equivalent to that for a 0.98 monolayer Ag. They are, however, unlikely because the adlayer–Au spacing clearly supports Ag atoms as the adsorbates. Pb atoms are about 20% larger than Au atoms, while Ag has nearly the same lattice constant as Au. The adlayer–substrate spacing obtained from the best fit is 2.36 Å, which is close to the Au(1 1 1) bulk spacing of 2.355 Å and far less than the Pb–Au layer spacing of 2.65 Å, found for the Pb UPD adlayer on Au(1 1 1) [16]. If a significant amount of Pb were in the adlayer, the adlayer–substrate layer spacing would be larger than the Au(1 1 1) bulk spacing, which would cause visible asymmetry in the reflectivity curve near the Bragg positions. The absence of this feature clearly supports the model with a pure Ag monolayer. The possibility of surface alloying, i.e., an Au–Ag place exchange, can also be ruled out based on the unity coverage for both the Au top layer and the Ag adlayer. This is because the fitted Ag coverage would be higher than unity and that of the top Au layer would be lower than unity as the electron density shifts from the top layer of the substrate to the adlayer by exchanging Au (electron-rich, $Z = 79$) with Ag (having a considerably smaller number of electrons, $Z = 47$).

To facilitate a comparison between the X-ray specular reflectivity profiles for our monolayer sample and for that obtained for the Ag UPD monolayer [12], a dashed line is shown in Fig. 3 which is calculated with the same parameters as those for the solid line except a lowered rms displacement amplitude for the Ag adlayer (from 0.45 to 0.15 Å). This curve is rather similar to that for the Ag UPD monolayer and thus indicates that there is a significant difference in subatomic scale between the two monolayer-films. We have found that the rms value for the Ag UPD monolayer on Pt(1 1 1) is 0.09 Å and in general the rms value for a UPD adlayer is less than 0.2 Å. Therefore, the high rms displacement amplitude likely originates from the deposition method.

For the Ag bilayer sample (Fig. 4), the characteristic feature in the specular reflectivity curve is the double dip between the origin and the (0 0 3) Bragg positions. The best fit (shown by the solid line) was obtained with $\theta_1 = 0.95$, $\theta_2 = 0.79$, and $\theta_3 = 0$. The layer spacings are 2.35, 2.36, and 2.39 Å for the top Au layer, the first and second Ag adlayers, respectively. Fittings with fixed nonzero third Ag layer coverage were carried out to see if other models also reproduce the reflectivity curve. A typical result is shown by the dashed line, which is obtained by fixing the coverage for the third Ag adlayer at 0.1, while allowing other parameters to vary. The third layer spacing (3.05 Å) and rms amplitude (1.2 Å) are both much higher than those for the first two layers, suggesting that there is no tightly bounded third Ag adlayer. The quality of the bilayer film is, however, quite different from that made by UPD. The fitted rms displacement amplitudes are 0.38 and 0.76 Å for the first and second Ag layers, respectively, significantly higher

than the those found for the Ag UPD bilayer on the Au(1 1 1) and Pt(1 1 1) surfaces [12,17]. The notable feature related to the large rms values is the absence of the double dip in the specular reflectivity curve between the (0 0 3) and (0 0 6) Bragg positions. In order to explore the reason for the higher rms values, a model that allows a small amount of Pb (which should have larger spacing than Ag) to be in the second adlayer was also used. With the layer spacings fixed at the ideal values, Au–Ag and Ag–Ag at 2.355 Å and Ag–Pb at 2.65 Å, a reasonable fit was obtained with the rms displacement amplitudes of 0.4 and 0.7 Å for the first Ag layer (0.97 ML) and the second Ag (0.76 ML)–Pb (0.03 ML) mixed layer, respectively. Since the rms value for the second layer is only slightly reduced in this model compared to that without any Pb (from 0.76 to 0.70 Å), the large rms value for the second adlayer cannot be fully accounted by a possible Ag–Pb mixed second layer. Similarly to the monolayer case, the rougher bilayer film compared to those obtained by UPD, is likely due to the lack of "annealing" effect of reversible adsorption–desorption under thermodynamic equilibrium, which helps the UPD adlayers to achieve a highly ordered state.

In addition to the potential cycling method described above, Pb mediated Ag depositions were also carried out at a fixed potential, where a partial Pb monolayer exists, and with potential pulses between the low and high limits of the Pb UPD potential region. These two methods were successfully employed in 2D growth of Ag films on Au(1 1 1) monitored with STM [6]. In the present study, we have had a limited success in making a complete overpotential deposited Ag monolayer by these two methods. The specular reflectivity profiles obtained from the three samples made by pulsing potential between −0.1 and 0.1 V failed to show layer-by-layer growth at monolayer level. For these deposits, two partial layers were required to fit the specular reflectivity profiles even the sum of the coverage for the two layers was equal to or less than one monolayer. These observations demonstrated that the uniformity of the film on an atomic scale is sensitive to the details on how the potential was controlled in the deposition procedure. This is not surprising because the OPD of Ag results in 3D islands in the absence of Pb ions and the layer-by-layer growth relies on a kinetic manipulation involving Pb UPD/stripping cycles. Since the smaller a 2D island is, the easier the adatom diffusion to its edge is, the mechanism of surfactant mediated growth is believed to involve a restraining the size of 2D nuclei to prevent growth of a new layer on the uncompleted growing monolayers. For the Pb mediated Ag deposition studied here, formation of large 2D Ag islands is blocked by co-deposition of Pb in the negative potential sweep. Stripping of the Pb monolayer in the positive potential sweep liberates those Pb-covered sites to allow further Ag–Pb co-deposition in the next potential cycle. Due to the continuous Ag OPD, Pb adatoms may be buried into the Ag film if the potential was kept negative of the UPD current peaks for an extended time. By using potential cycles to repeatedly deposit and remove Pb, Ag–Pb place exchange is effectively enhanced. All these effects depend on the experimental detail, so does the quality of the mediated 2D growth.

4. Conclusions

Layer-by-layer OPD of Ag monolayer and bilayer on Au(1 1 1) mediated by Pb UPD/stripping cycles was investigated in order to explore the methods for enhancing 2D growth of ultra-thin metal films under OPD conditions. As demonstrated by the X-ray specular reflectivity measurements, nearly complete monolayer and bilayer films can be made with optimized deposition procedures. These results indicate that the 2D growth is enhanced through blocking the formation of large Ag islands at low coverage by the co-adsorption of Pb, and through enforced place exchange during Pb stripping processes. Both effects keep the interlayer transport of deposited Ag adatoms rapid enough to prevent nucleation of islands on the as yet uncompleted growing monolayer. On subatomic scale, however, for films obtained using this procedure we found that it is rather difficult to match the smoothness of thin films made by UPD.

Acknowledgements

This work is supported by US Department of Energy, Divisions of Chemical and Material Sciences, under the contract no. DE-AC02-98-CH10886.

References

[1] M. Copel, M.C. Reuter, M. Horn-von Hoegen, R.M. Tromp, Phys. Rev. B 42 (1990) 11682.
[2] M. Horn-von Howgen, F.K. LeGoues, M. Copel, M.C. Reuter, R.M. Tromp, Phys. Rev. Lett. 67 (1991) 1130.
[3] G. Meyer, B. Voigtlander, N.M. Amer, Surf. Sci. 274 (1992) L541.
[4] H.A. van der Vegt, H.M. van Pinxteren, M. Lohmeier, E. Vlieg, J.M.C. Thornton, Phys. Rev. Lett. 68 (1991) 3335.
[5] G. Rosenfeld, R. Servaty, C. Teichert, B. Poelsema, G. Comsa, Phys. Rev. Lett. 71 (1993) 895.
[6] K. Sieradzki, S.R. Brankovic, N. Dimitrov, Science 284 (1999) 138.
[7] J.D.E. McIntyre, W.F. Peck, J. Electrochem. Soc. 123 (1976) 1800.
[8] D. Davidović, R.R. Adžić, Electrochim. Acta 33 (1988) 103.
[9] N.S. Marinkovic, J.X. Wang, J.S. Marinkovic, R.R. Adžić, J. Phys. Chem. B 103 (1999) 139.
[10] R.R. Adžić, in: H. Gerischer (Ed.), Adv. Electrochem. & Electrochem. Eng., vol. 13, J. Wiley & Sons, New York, 1984, p. 159.
[11] M.J. Esplandiu, M.A. Schneeweiss, D.M. Kolb, Phys. Chem. Chem. Phys. 1 (1999) 4847.
[12] T. Kondo, J. Morita, M. Okamura, T. Saito, K. Uosaki, J. Electroanal. Chem. 532 (2002) 201.
[13] C.H. Chen, S.M. Vesecky, A.A. Gewirth, J. Am. Chem. Soc. 14 (1992) 451.
[14] D.M. Kolb, in: R.C. Alkire, D.M. Kolb (Eds.), Advances in Electrochemical Science and Engineering, vol. 7, Wiley VCH, Weinheim, Germany, 2002, p. 107.
[15] M.F. Toney, J.G. Gordon, M.G. Samant, G.L. Borges, O.R. Melroy, D. Yee, L.B. Soresen, J. Phys. Chem. 99 (1995) 4733.
[16] Unpublished results.
[17] J.X. Wang, N.S. Marinkovic, R.R. Adžić, B.M. Ocko, Surf. Sci. 398 (1998) L291.